Journal of Inorganic Biochemistry 198 (2019) 110714

Contents lists available at ScienceDirect

Journal of Inorganic Biochemistry

journal homepage: www.elsevier.com/locate/jinorgbio

The electrochemical profiles of Auranofin and Aubipy^{c}, two representative medicinal gold compounds: A comparative study

Monika Kupiec[a], Robert Ziółkowski[b], Lara Massai[c], Luigi Messori[c], Katarzyna Pawlak[a,*]

[a] Chair of Analytical Chemistry, Faculty of Chemistry, Warsaw University of Technology, Noakowskiego 3, 00-664 Warsaw, Poland
[b] Chair of Medical Biotechnology, Faculty of Chemistry, Warsaw University of Technology, Noakowskiego 3, 00-664 Warsaw, Poland
[c] Department of Chemistry, University of Florence, 50019 Sesto Fiorentino, Florence, Italy

ARTICLE INFO

Keywords:
Cytotoxic gold complexes
Metallodrug
Prodrug
Electrochemical cell
Voltammetry
Electrospray MS

ABSTRACT

A micro-electrochemical reaction cell was coupled to an electrospray mass spectrometer in order to track redox transformations for two representative medicinal gold compounds - *i.e.* [(2,3,4,6-tetra-*O*-acetyl-1-thio-*β*-D-glucopyranosato-S)(triethylphosphine)gold(I)] and [Au(bipy^{dmb}-H)(OH)][PF_6] (where bipy^{dmb}-H is deprotonated 6-(1,1-dimethylbenzyl)-2,2′-bipyridine), known as Auranofin and Aubipy^{c} respectively - in parallel to square wave voltammetry (SWV) measurements. Irreversible oxidation of thio-glucose tetraacetate was the dominant reaction for the gold(I) compound Auranofin; oxidation was accompanied by hydrolysis leading to progressive deacetylation. Two main active forms were identified for this prodrug: the triethylphosphinegold(I) cation and a gold(I) thioglucose species, with a variable number of acetyl groups. For the gold(III) complex Aubipy^{c} irreversible reduction of the gold(III) center was highlighted, accompanied by a ligand exchange process. The free gold(I) ion is proposed to be the final species that subsequently binds transport proteins in the bloodstream. Molecule specific mass spectrometry determinations provide complementary data to square wave voltammetry helping to understand the nature of the electrochemical conversions of complex or unstable compounds. Finally, it was possible to establish that oxidizing conditions during drug preparation and administration should be avoided in the case of Auranofin; conversely, reduction conditions typical for the blood or the cytosol environment are suitable to obtain the active gold(I) species from the gold(III) complex Aubipy^{c}.

1. Introduction

Cisplatin, one of the leading anticancer metallo-drugs is known to produce stable DNA adducts. This is the accepted basis for its potent antitumor actions and its worldwide use. Despite its large clinical success, there are several disadvantages associated with the use of cisplatin, such as low solubility and relevant toxicity (which limits patient doses), severe side effects, and intrinsic or acquired resistance in numerous cancer types [1]. Therefore, the development of novel metallodrugs with different mechanisms of action is a main goal for modern medicinal inorganic chemistry [2]. Indeed, several metal complexes, mainly combining the unique character of unusual and non-physiological metal centers with a variety of organic ligands, were found to exhibit promising pharmacological properties often relying on modes of action deeply distinct from those of platinum compounds [3]. Various gold(I) and gold(III) complexes belong to a group of rapidly emerging novel therapeutic and diagnostic metal complexes with improved specificity for tumor tissue and with remarkable antiproliferative potency [4]. They are usually responsible for drastic cancer growth inhibition related to mitochondrial activation of cancer cell apoptosis. Yet, the mechanism of action for gold-based drugs is poorly understood. Auranofin – a well-known second generation gold(I) complex – shows an increased cell membrane solubility associated to the presence of the phosphine ligand. Pairwise, it was reported and postulated that gold complexes can inhibit the enzymatic activity of TrxR (Thioredoxin Reductase) [5], ribonuclease A (RNase A), deoxyribonuclease I (DNase I) [6] or react with zinc finger domains [7] leading to relevant cellular perturbations.

It should be stressed that metal complexes are, usually, pro-drugs, that are metabolized to their pharmacologically active species after administration to the patient [8]. Transformations of metallo-drugs can influence the efficiency of their absorption, distribution, metabolism and excretion (ADME). Consequently, characterization of their stability and of the possible metabolites is crucial for understanding their mode of action and for predicting optimal doses in patients, the likely side effects, their stability and impact on the environment. Finally, the

* Corresponding author.
E-mail address: kasiap@ch.pw.edu.pl (K. Pawlak).

https://doi.org/10.1016/j.jinorgbio.2019.110714
Received 4 December 2018; Received in revised form 9 May 2019; Accepted 13 May 2019
Available online 28 May 2019
0162-0134/

identification of the active forms of metallo-drugs can help to create more effective next generation ones, and this is very challenging, especially for transition metals derivatives.

To explore the redox chemistry of metallodrugs under biological relevant conditions, electrochemical techniques are often used to determine the redox potential of the various metallodrugs in comparison to components of the cytosol (from −0.8 to +0.8 V) [9] or of the blood (from −0.05 to +0.05 V) [10], to identify the oxidative products of drugs administered orally [11] or extrinsically (up to +1.7 V) [12] or to establish the ability of the investigated compounds to create reactive oxygen species (from −1.6 to +2.5 V) [13]. Usually, two methods are employed: cyclic voltammetry and square wave voltammetry [14]. Both of them allow studying the reactivity of metal-based compounds combined with the movement of electrons in respect to changed potential. The significance of electrochemical methods and their widespread applicability is worldwide appreciated. However, their application is often limited to non-complex redox reactions due to insufficient selectivity even when powerful tools are applied to analyze data *e.g.* multivariate curve resolution (MCR) [15]. Both redox and interfering reactions (for example hydrolysis) can be traced by coupling the electrochemical reaction cell (EC) with electrospray ionization mass spectrometry (ESI-MS). Coupled EC/ESI-MS was mainly used to obtain oxidation products of different compounds, for example, to improve the sensitivity of ESI-MS quantitation methods [16,17]. We assumed that electrochemical mass spectrometry can provide valuable results on the redox chemistry of selected metal transition complexes which exhibit favourable antitumor activity profiles. Thus, the aim of this study was to use an electrochemical microcell as a redox reactor with on-line ESI-MS detection to study the transformations of a few representative gold complexes.

Two gold(I)/(III) perspective and analytically challengeable metallo-drugs were chosen to evaluate EC/ESI-MS as an approach suitable to reveal the activity of selected complexes and to identify their potential active metabolites required in early stages of drug development.

We have focused our attention on Auranofin [(2,3,4,6-tetra-*O*-acetyl-1-thio-*β*-D-glucopyranosato-S)(triethylphosphine)gold(I)], (Fig. 1A-B), an established gold(I) drug, and on Aubipy^{c}, the cyclometallated gold(III) hydroxo complex [Au(bipy^{dmb}-H)(OH)][PF_6] (where bipy^{dmb} -H is deprotonated 6-(1,1-dimethylbenzyl)-2,2′-bipyridine). Auranofin consists of two main parts: the water-soluble aurothioglucose portion with the S donor group and the phosphine ligand responsible for the lipophilic character of this gold(I) compound. The linear S-Au-P geometry characterized by X-ray crystallography [18] was found to be suitable for exchange reactions with biological ligands. Auranofin is in clinical use since the 1980s for the treatment of rheumatoid arthritis; it is currently the object of repurposing in cancer and various infectious and parasitic diseases. It is now ascertained that Auranofin exerts potent antineoplastic activity in various *in vitro* and *in vivo* tumor models [19]. Owing to the observation of favourable anticancer effects *in vivo* [20,21], Auranofin during the last years has entered three distinct clinical trials: ovarian cancer, lung cancer and leukemia, the latter already closed [22–24]. It also represents a reference compound when new gold-based compounds are studied as potential anticancer drugs, although the mechanism of action of Auranofin in cancer is not fully understood.

On the other hand, Aubipy^{c} is a promising gold(III) compound that was extensively characterized, both chemically and biologically, through a few studies [25,26]. Aubipy^{c} consists of a square planar gold (III) centre receiving three donor atoms –*i.e.* C,N,N- from the terdentate bipyridyl ligand while the fourth coordination position is occupied by a hydroxide group, the latter being the preferential site for ligand replacement reactions and for protein binding. Aubipy^{c} is acceptably stable under physiological conditions. The compound was tested against a panel of 12 cancer cell lines and reported to produce significant antiproliferative effects [27]. Some valuable mechanistic

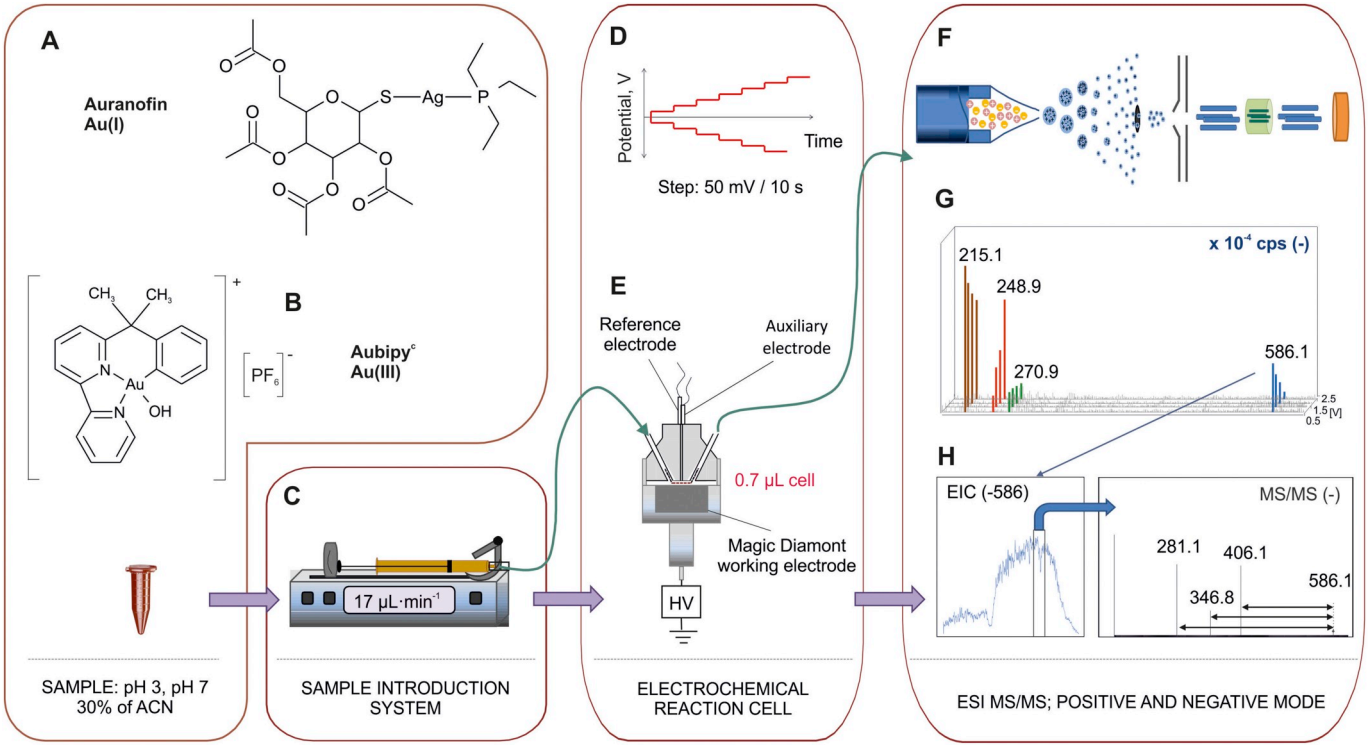

Fig. 1. Schematic presentation of analytical protocol for EC-MS^2 experiments.

Table 1
Parameters applied for EC/ESI-MS coupling and squared wave voltammetry (SWV).

Parameter	EC	SWV
Cell volume, µL	0.7 µL	N/A
Working electrode	Magic Diamond – The diamond deposited on a silicon carrier	Glassy carbon disk electrode
Reference electrode	Ti based electrode with potential relative to Pd/H_2	$Ag/AgCl/1.0\ mol\ L^{-1}$ KCl
Oxidation potential range, V	0–3.5	-0.7–1.8
Reduction potential range, V	−2.5–0	
Sweep rate, $V\ s^{-1}$	0.1	0.1
Dwell time, s	10	2
Flow rate, $\mu L \cdot min^{-1}$	17	N/A
Pulse amplitude (increment), V	N/A	0.025 (0.004) with 15 Hz frequency

Electrospray mass spectrometry	
Ionization voltage, kV	2500 (positive ion mode) 1500 (negative ion mode)
Orifice voltage, V	500
Nebulizing gas flow, L/min	7
Nebulizing gas pressure, psi	40
Nebulizing gas temperature, °C	300
Drying gas flow	7
Drying gas temperature	250
Fragmentor voltage, V	90
Monitored mass ranges, m/z	0–700 and 500–1200 for Auranofin, 0–800 for Aubipy[c]
Dwell times, ms	100
Acquisition step, m/z	0.1
Collision energies, eV	20, 30, 40

insight was obtained by proteomic studies [28]. However, several aspects of its mode of action remain unexplored and warrant further studies.

2. Material and methods

2.1. Chemicals

[Au(III)($bipy^{dmb}$-H)(OH)][PF_6], where ($bipy^{dmb}$-H is 6-(1,1-dimethylbenzyl)-2,2′-bipyridine) known as Aubipy[c] was synthesized and purified according to previously published protocol [25]. Auranofin (≥98% purity) and other reagents were obtained from Sigma-Aldrich (St. Louis, USA) and used as received in this study. Structures of both complexes are presented in Fig. 1A. Acetonitrile (ACN, LC-MS purity) from Avantor Performance Materials Poland S.A. and deionized water from a Milli-Q system (Millipore Elix 3, Saint-Quentin, France) were used throughout the experiments.

2.2. Sample preparation

Stock solutions of studied metal compounds $1{\cdot}10^{-4}$ M were prepared by dissolving of an appropriate amount of powder in dimethyl sulfoxide (DMSO). Obtained solutions were diluted twice with 100 mM tetrabutylammonium tetraphenylborate solution prior voltammetric experiments. Prior to EC/ESI-MS experiments, stock solutions were diluted 10 times in aim to obtain $1{\cdot}10^{-5}$ M aqueous solutions of complexes containing 30% ACN and: (A) 0.1% formic acid or (B) 10 mM ammonium formate pH 7.4 (Fig. 1A).

All solutions were protected from light, the solution of Aubipy[c] was kept in the fridge for maximum 10 days. Auranofin solution was prepared just before experiments.

2.3. Square wave voltammetry

Voltammetric experiments were performed with a CHI 660A electrochemical workstations (CH Instruments, USA). The measurements were recorded with a conventional three-electrode system including a glassy carbon disk electrode (CH Instruments, USA), an Ag/AgCl/1.0 M KCl reference electrode and a gold wire auxiliary electrode. Sweep rate $0.1\ V\ s^{-1}$ with 2 s quiet time was applied. Gold(III) complex due to low sensitivity of voltammetry was enriched by immersion of 10 µL solution containing gold complex ($5{\cdot}10^{-5}$ M) and tetrabutylammonium tetraphenylborate on the working electrode and evaporation in the dark (3 h).

2.4. Electrochemical reaction cell (EC)

All EC/ESI-MS experiments were performed by means of ROXY EC system (Antec, The Netherlands) consisting of a potentiostat, equipped with an electrochemical micro-reactor cell (µ-PrepCell, Antec, The Netherlands) and an infusion pump (KD scientific, model KDS100, USA, Fig. 1C). The Roxy system was online hyphenated to an Agilent 6460 LC/MS ESI triple quadrupole mass spectrometer (Santa Clara, USA) as a detector. A schematic drawing of the instrumental set-up used for experiments is presented in Fig. 1E. Electrochemical red-ox reactions were performed in the µ-PrepCell. This thin-layer electrochemical reactor cell consisted of a diamond-based working electrode, reference electrode and inlet block of the cell employed as a counter electrode. A 50-µm spacer was used to separate electrodes giving a cell volume of 0.7 µL. The ROXY EC system was controlled by Dialogue software (Antec, The Netherlands). An electrical grounding union and additionally 30 cm long transfer line connecting EC with ESI nebulizer was used to decouple the electrochemical circuit from the ESI source [29]. The connections were made of PEEK tubing (0.13 mm i.d.). The electrochemical cell was thermostated to 35 °C. For each complex electrochemical reaction was performed with step 50 mV per 10 s (Fig. 1D) and three series of measurements were carried out for negative and positive potentials. Potentials applied to the working electrode in EC were starting always from 0 V to maximum of positive or negative potentials for easier recognition of signals corresponding to redox reaction products and to decrease the time of the analysis. The syringe was refilled with a fresh solution before each analysis.

In the case of both complexes significant changes of signals intensity were observed only at pH 7.4 and discussion of the results refers only to these conditions.

2.5. Electrospray ionization mass spectrometry (ESI-MS)

ESI-MS detection for EC was performed in positive (2500 V) and negative (1500 V) ion mode. For each complex, optimization of mass spectrometric conditions was accomplished by direct infusion of the complex at flow 17 μL/min. Positive and negative ionization, fragmentor voltages, nebulizing gas flow and pressure were established as 2.5 kV, 1.5 kV, 90 V, 7 L/ min and 40 psi, respectively. Acquisition of ions was carried out with 0.1 *m/z* step and 100 ms dwell time in m/z ranges appropriate for the molecular mass of investigated complexes. Three collision energies 10, 20 and 30 eV were applied toward fragmentation of selected ions. For instrument control, Mass Hunter Workstation software (Agilent Technologies) was used.

All detection parameters are presented in Table 1.

2.6. Data analysis

The preliminary form of ESI-MS data was total ion chromatogram (TIC) obtained for positive and negative ionization mode separately (due to refilling of the syringe with fresh solution). In the first step, mass spectra were obtained for the average voltage applied during 0.5 min (step 0.3 V) to the working electrode. Next, they were subtracted with mass spectra obtained for blank solution at the same electrochemical potential and ESI detection parameters (Fig. 1G) using the Agilent Mass Hunter Qualitative Analysis B.05.00 software (Agilent Technologies). Signals present in the subtracted mass spectra were selected toward extraction of ion chromatograms (EIC, Fig. 1H) and better recognition of start point for redox reaction and potential range toward ESI-MS/MS experiments.

ESI-MS/MS mass spectra for different collision energies were summed up to obtain rich mass spectra for its efficient interpretation and to reveal the structure of parent ion.

3. Results and discussion

3.1. The redox profile of gold complexes by square wave voltammetry

3.1.1. Auranofin

Three irreversible redox processes were found at all scan rates, concentrations, and switching potentials investigated. The first (+0.40 V) one can be described as sulfur-based oxidation, the second or the third (+0.75 and +1.25 V) one can correspond to the rearrangement of the phosphine gold complex leading to the formation of clusters accompanied by the change of the gold oxidation state into a higher one (Fig. 2A). All three potentials do not correspond to published data obtained *via* cyclic voltammetry (+1.1 and +1.6 V) using CH_2Cl_2 as the solvent [30]. Shifts in potential values can be observed due to changes of working and reference electrode, pH of the solution, solution composition or ligand complexing metal ion. For example, application of a water mixture with acetonitrile instead of CH_2Cl_2 changes the three last factors. Additionally, the nitrile group (a common food metabolite) is also known to be a strong complexing agent for Au^+. The formation of $[Au(CN)_2]^-$ was proposed as one of the key metabolites for gold-based drugs [31]. This complex was detected in the urine of patients treated with Auranofin.

3.1.2. Aubipy^c

The first peak at the potential of −0.8 V was observed only during the first anodic process. It was possible to regain the peak after 30 min dwell time between cycles (Fig. 2B). Such influence of the kinetics of the process during SWV experiments can be related to the reorganization of the complex molecules on the surface of the electrode controlled by diffusion. Cathodic SWV peaks observed at −0.35, −0.60, −0.68 and − 0.76 V can correspond to reduction of gold. Shifts in cathodic potentials in the range − 0.60 - −0.76 V can be the result of irreversible changes in the ligand structure [32,33], but it can be also related to poor efficiency of non-homogeneous deposition of the gold complex on the surface of the electrode.

Results obtained by SWV indicate that the oxidation state of gold affects the redox activity of the complex: SWV promotes oxidation for Au(I) and reduction for Au(III) complex.

3.2. Examining the redox activity of gold complexes by EC/ESI-MS/MS

As ESI-MS detection is used for EC, the signal intensity depends on several additional factors due to the characteristics of the compound, such as pK_a, molecular mass, and complexity of the isotopic pattern specific for each compound and influence of sodium ions [34]. Additionally, constant addition of the sample to the microEC cell and a high concentration, suitable for ESI-MS, of the investigated compounds in comparison to small surface of the working electrode can influence the kinetics of the reaction. It can lead to asymmetric peaks in MS voltammograms. Due to that, the reversibility of the processes carried out by EC/ESI-MS cannot be discussed analogically to square wave voltammetry. Moreover, during sample administration (for 10–12 min), hydrolysis of metal complexes can take place in water solution or additional redox reactions in the electrospray chamber. This may be the reason for the presence of signals corresponding to products of:

1) electrochemical redox reactions,
2) hydrolysis,
3) secondary redox reactions in the ESI source,
3) the combined reactions mentioned above.

It should be also mentioned that due to the application of different reference electrodes, shifts for the electrochemical potential can be expected.

3.2.1. Auranofin

The identity of compounds related to selected signals was established by careful analysis of the fragmentation spectra (Fig. 3, Table 2). EC reactions were analysed, in function of the time, following the change of intensity of selected signals due to the variation of potential (EIC as MS voltammograms).

During the EC/ESI-MS experiments, the negative potential applied to the working electrode was found to stabilize the gold ion simultaneously bound to sulfur and phosphorus. Signals at *m/z* + 701, +679, +659 and + 617 corresponding to sodiated, protonated and partially deacetylated ions of Auranofin (Table 2) were observed in the wide range of potentials from −2.5 to 1.5 V. The signal at m/z + 433 corresponding to $[Au^I(tEP)_2]^+$ was also increasing at negative EC potentials. However, the intensity of the signal observed at *m/z* − 229 corresponding to the doubly-charged ion formed by $[Au^I(tEP)_2]^+$ and nitrile group was too low to observe the same correlation to electrochemical voltage.

Average potentials were also found to stabilize Au^I-S and Au^I-P. For example, signals observed at *m/z* + 281 and + 659 corresponding to $[tetraAtgS\text{-}Au^I + 2H^+]^{2+}$ and $triAtgS\text{-}Au^I\text{-}tEP$ (where AtgS is acetyl-1-thio-β-D-glucopyranosato-S group and tEP is triethylphosphanium one), respectively, were significantly higher in the range of potentials −1.5–1.0 V (Fig. 4). Another signal, higher in the range 0.2–3.0 V, was observed for ion at *m/z* + 175. It corresponds to double-charged ion and was subjected to MS/MS analysis. Two fragmentation ions were only observed, but only for even m/z values. This indicates the presence of the nitrogen atom. Fragmentation ion at m/z + 130 can correspond to tEP = NH group and + 116 is obtained through the loss of CH_4. It is possible that this compound is an artifact formed due to the presence of acetonitrile, which prevents the formation of most probable triethyl phosphine oxide (tEP = O, M = 134) reported by Albert [31]. It may happen because of the lack of competitive ligand or too long reaction time for oxidation. When glutathione was added to the solution containing Auranofin (molar ratio 1:1) the small signal at *m/z* + 135 was observed at potential higher than 0.2 V. The signal corresponding to tEP = O was also obtained when methanol was used instead of

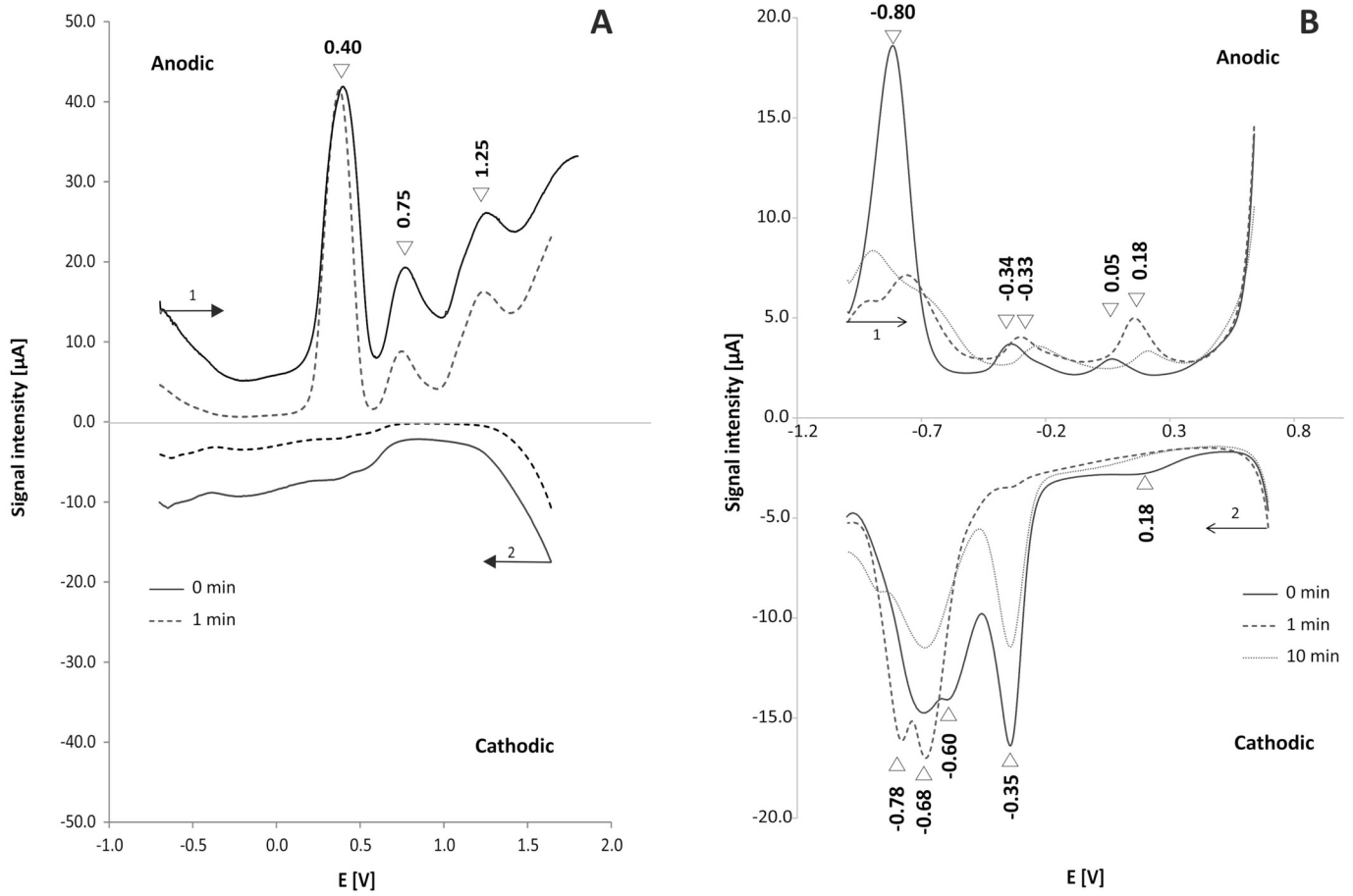

Fig. 2. Squared wave voltammogram obtained for A: 50 µM auranofin in the mixture of 10 mM ammonium formate pH 7.4 and for B: 10 µL of 50 µM Aubipy^c in the mixture of 10 mM ammonium formate pH 7.4 in water and ACN (70:30) with 100 mM tetrabutylammonium tetraphenylborate. Aubiy^c was enriched on the working electrode.

acetonitrile and acetic acid instead of formic acid. Unfortunately, signal-to-noise decreased 10 times when methanol was used. Acetic acid, when used, caused the formation of bubbles in the electrochemical chamber which disturbed aerosol formation. Yet, it should be stressed that during all three experiments signal at m/z + 175 was not observed.

The main products of the anodic process were observed as signals at m/z − 249 and + 364 corresponding to deprotonated and protonated dimer of thioglucopyranose with disulfide bridge $[(\text{tetraAtgS})_2 + Na^+ - 4H^+]^{3-}$ and $[(\text{tetraAtgS})_2 + 2H^+]^{2+}$, respectively. The third main signal was observed at m/z − 586 and corresponds to complex obtained *via* exchange of tEP by nitrile group from acetonitrile ($[\text{tetraAtgS-Au-CN}]^-$. Careful comparison of intensity alterations was carried out for these three signals against the potential. It was found that the first signal, which starts to increase at potential ~0.3 V, is −586 and it reaches a plateau at 0.5 V. Maximum of intensity observed at +2.3 V and sudden signal drop suggests that $[\text{tetraAtg-Au-CN}]^-$ is an intermediate product from which $(\text{tetraAtgS})_2$ is formed. A similar effect can be observed in the presence of the sodium cation, which enhances the formation of disulfide bridges [35].

It should be also reported that noise level in extracted ion chromatogram was increasing for higher negative potentials. This effect can correspond to the formation of clusters by gold complex [36,37] with bridging thiolate ligands (based on X-ray studies [38]) or triethyl phosphine [39].

Reduction and intermediate electrochemical conditions corresponding to redox conditions of cytosol and blood were found optimal to obtain the most probable reactive forms for Auranofin: $(\text{tEP})_2$-Au and tetra(tri and di)AtgS-Au, which can interact with biomolecules in the human organism. The proposed identities of obtained products are in agreement with those reported by Albert [31]. Products of deacetylation were insignificant and were mainly observed in the presence of sodium cations. This is consistent with the described ability of sodium hydroxide to enhance the kinetics of this reaction [40]. Deacetylation and loss of Atg or tEP groups by Auranofin are irreversible processes as is disulfide formation. Nitrile group attaching to gold and its influence on the transformation of Auranofin, may mimic, to some extent, the ligands behaviour under physiological conditions. Ligand exchange can be proposed as the most probable mechanism for metabolic changes of Auranofin.

Two main oxidation products of Auranofin were discovered by EC/ESI-MS: oxidized tEP and dimer of tetraacetyl-1-thio-β-D-glucopyranosato-S group (Fig. 5), which was obtained from Auranofin and for higher potential from $[\text{tetraAtg-Au-CN}]^-$. Squared wave voltammogram also consisted of three peaks. Yet, potentials differ significantly, and a direct comparison of the results obtained by two discussed techniques is not possible. SWV peaks can be only assigned to identified molecules following the order of peaks obtained by EC/ESI-MS during the anodic process.

3.2.2. Aubipy^c

Signals for analysis were selected and identified following the same protocol used for Auranofin. However, the gold(III) complex is positively charged and signals in negative ion mode of ESI-MS were not observed (Fig. 6, Table 3).

The signal at m/z + 527 was recognized as the hydrolysis product of investigated gold(III) complex. Similarly to Auranofin, hydrolysis was

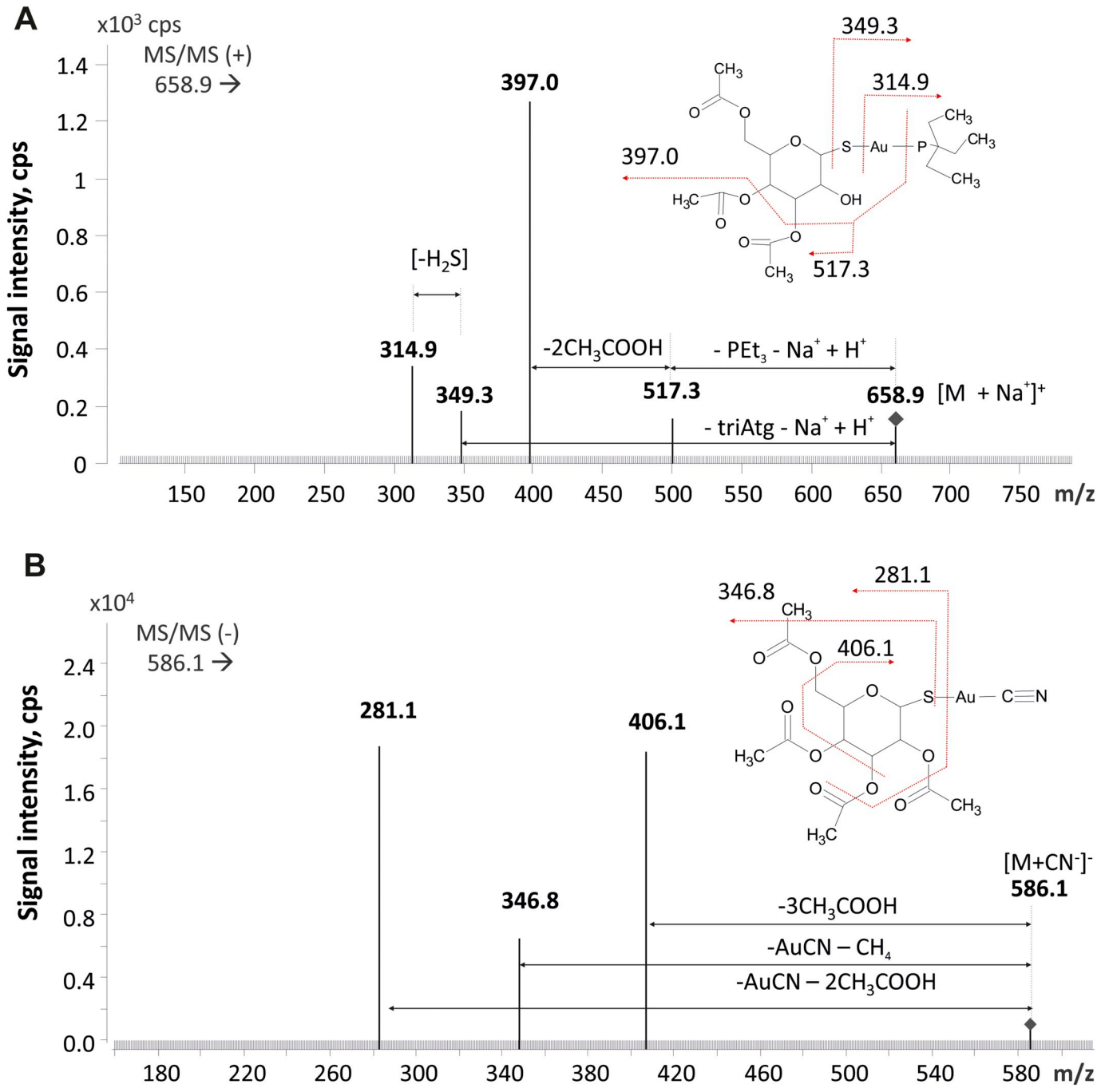

Fig. 3. EC/ESI-MS^2 mass spectra for auranofin parent ions at *m/z* 659 (A) and m/z 586 (B).

found to be promoted by the anodic process and by the presence of sodium ions [41]. For higher EC potentials (2.7–3.5 V), two peaks were observed in the extracted ion chromatogram for signals observed at *m/z* + 273 and +517. The first signal corresponds to ligand (biPYisoPB, where biPY is bipyridine and isoPB is isopropylobenzen group, Table 3) with a mass lower by 2 u due to loss of H_2 (oxidation) during formation of the new bond. Such an effect is usually observed when the metal ion is released from molecule. The second peak observed for m/z + 517 corresponds to the complex with the attached nitrile group (Table 3). Yet, the proposed structure should be verified by other technique.

In the range of −0.8–2.0 V two pairs of overlaid peaks were observed for signals +433 with +364 and +226 with +157. The ion at *m/z* + 433 was fragmented to identify the hypothesized structure. Among fragmentation ions, there was no signal corresponding to the gold ion at m/z + 197 and +66, for z equal 1 and 3, respectively (Fig. 6A, Fig. 7). This means that the observed signal is related to the ligand with even number (odd *m/z* value) of nitrogen atoms, which can be easily protonated (Table 3). Fragmentation signals and loss of neutral isoPB molecule lead to the conclusion that with loss of the gold ion, a bipyridine dimer is formed (reduction product) with one isoPB group attached (Fig. 6A). The ability of the ligand to release isoPB group is also confirmed by the presence of a signal corresponding to bipyridine cation (*m/z* + 157, Table 3). In the same range of potential (0.1–2.0 V), two signals corresponding to compounds containing the gold ion were observed. The signal at m/z + 364 can correspond to the Au(III) complex obtained *via* loss of one pyridine (PY) group and H_2 - $[Au^{III}=PYMB]^+$ or *via* reduction of gold ion - $[Au^{I}\text{-}PYMB]^+$, where MB refers to methylbenzene. The second hypothesis seems to be more

Table 2
Proposed identities for signals observed by EC/ESI-MS for auranofin.

Auranofin, tetraAtgS-Au^{I}-tEP; M = 678.48, M_{mi} = 678.13 g/mol

m/z	Fragmentation ions	Proposed formula	M^*_{exp}	$M^*_{theoret.}$	ΔM [ppm]
Signals with constant intensity					
+679	N/D	$[tetraAtgS\text{-}Au^{I}\text{-}tEP + H^+]^+$	678.10	678.14	59
+701	315, 397, 499	$[tetraAtgS\text{-}Au^{I}\text{-}tEP + Na^+]^+$			
+617	318	$[diAtgS\text{-}Au^{I} + Na^+]^+$	594.00	594.09	152
−281	N/D	$[(tetraAtgSH)_2Au_2 - 4H^+]^{4-}$	1120.00	1120.08	71
−229	N/D	$[Au^{I}(tEP)_2(CN^-) - H^+]^{2-}$	433.18	433.15	69
−215	35, 97, 117, 313	$[Au^{I}(tEP)_2 - 3H^+]^{2-}$	433.18	433.15	69
+433	61, 89, 117, 287, 315	$[Au^{I}\text{-}(tEP)_2]^+$	433.10		115
Zone I (−1.3–1.3 V)					
+659	315, 350, 397, 517	$[triAtgS\text{-}Au^{I}\text{-}tEP + Na^+]^+$	636.20	636.10	137
+281	109, 121, 131, 149, 347, 406	$[tetraAtgS\text{-}Au^{I} + 2H^+]^{2+}$	560.40	560.04	643
+175	116, 130	$[(PEt_3OPEt_3)_2^+(CN^-)_2 + 2Na^+]^{2+}$	304.18	304.16	66
Zone II (1.3–3.5 V)					
−725	N/D	$[(tetraAtgS)_2 - H^+]^-$	726.10		35
+364	281, 413, 453, 557	$[(tetraAtgS)_2 + 2H^+]^{2+}$	726.20	726.15	69
−249	45, 93, 169	$[(tetraAtgS)_2 + Na^+ - 4H^+]^{3-}$	726.20		69
−586	281, 347, 406	$[tetraAtgS\text{-}Au^{I}\text{-}CN^-]^-$	586.04	586.05	17

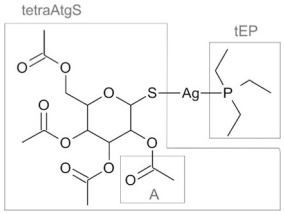

tetraAtgS - tetraacetyl-1-thio-β-D-glucopyranosato-S group; tEP – triethylphosphanium group; tri/diA – tri/diacetyl group; N/D – not detected, ΔM – established as a ratio $|M^*_{exp.}\text{-}M^*_{theorit.}|/M^*_{theorit.}$ *Monoisotopic mass of molecule - M_{mi}, Molecular mass – M

probable, especially upon considering that in the same potential range (0.1–1.4 V) a peak for signal *m/z* + 226 is observed which was identified as Au^{I}-CH = NH. Both forms suggest that the active form of the drug is Au^+, which can attach to biomolecules present in blood or cytosol. This observation is in agreement with Gabbiani's interpretation of ESI-MS results when considering the interactions of Aubipy[c] with cytosolic proteins [26]. Moreover, the gold(I) ion is more probable as an active form than complex with strong steric influence. It is possible that in the range of potentials from −0.8 to 0.05 V three different reactions can take place: reduction of gold in complex $Au^{I/III}$biPYisoPBOH, reduction of the ligand (signal m/z 433) and reduction of gold combined with the exchange of ligand by nitrile group. The scheme of transformation for Au^{III}biPYisoPBOH complex is presented in Fig. 8.

In the case of the EC/ESI-MS experiments carried out for Aubipy[c], the observed signals were generally higher and peaks sharper. Only EIC peak obtained for the signal at m/z 527 was wider and noisier, similarly

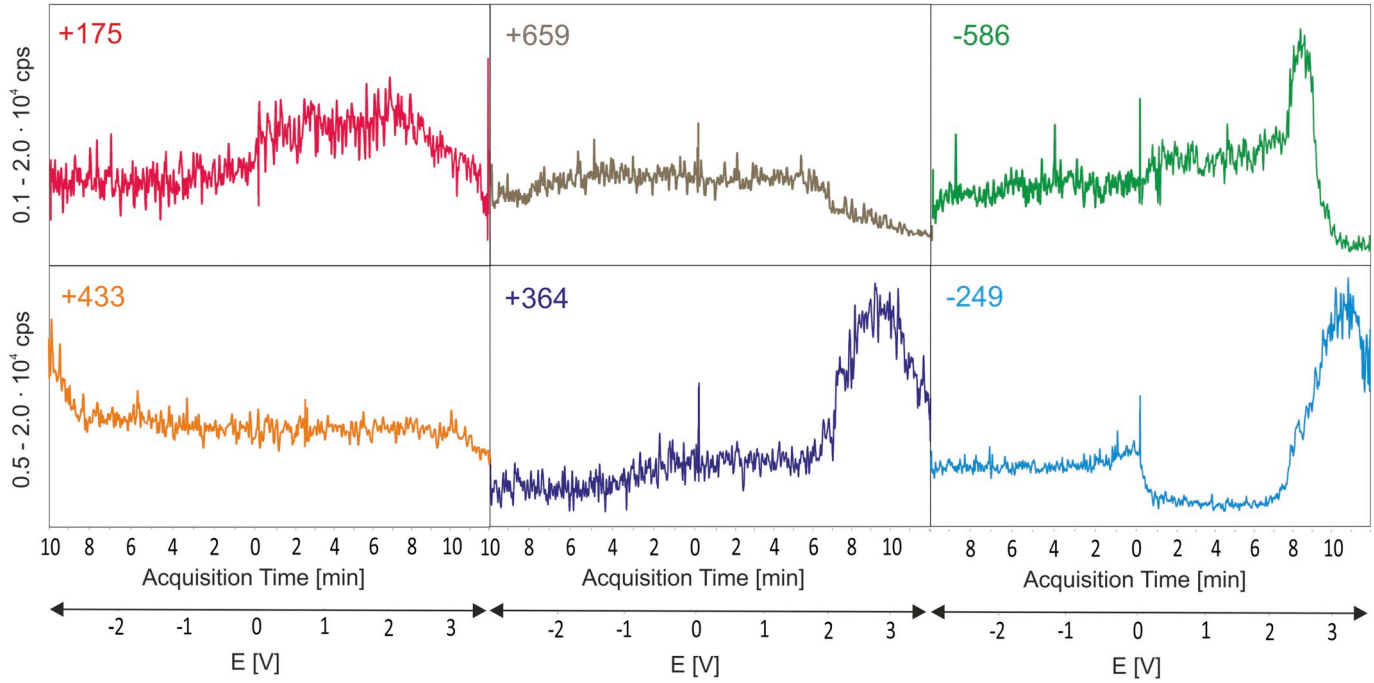

Fig. 4. Mass spectrometric voltammograms of selected ions (not smoothed extracted ion chromatograms, EICs) obtained by EC/ESI-MS for 10 µM auranofin in the mixture of 10 mM ammonium formate pH 7.4 in water and ACN (70:30).

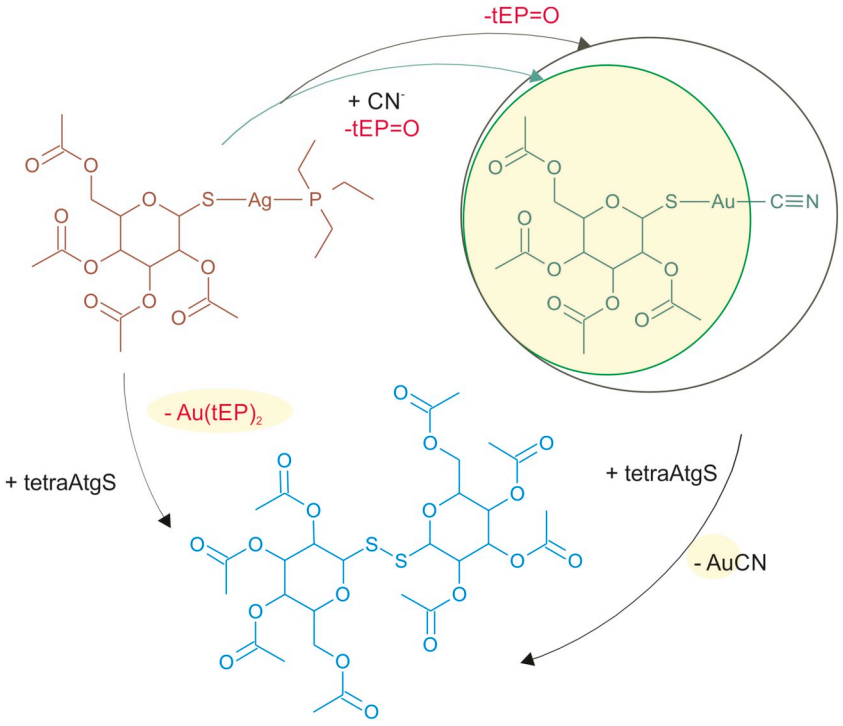

Fig. 5. Transformation of auranofin obtained by EC/ESI-MS. Structures with yellow background are proposed as the most probable active forms of the investigated prodrug. Colors of drawings correspond to colors of mass spectrometric voltammograms present in Fig. 4. (For interpretation of the references to color in this figure legend, the reader is referred to the web version of this article.)

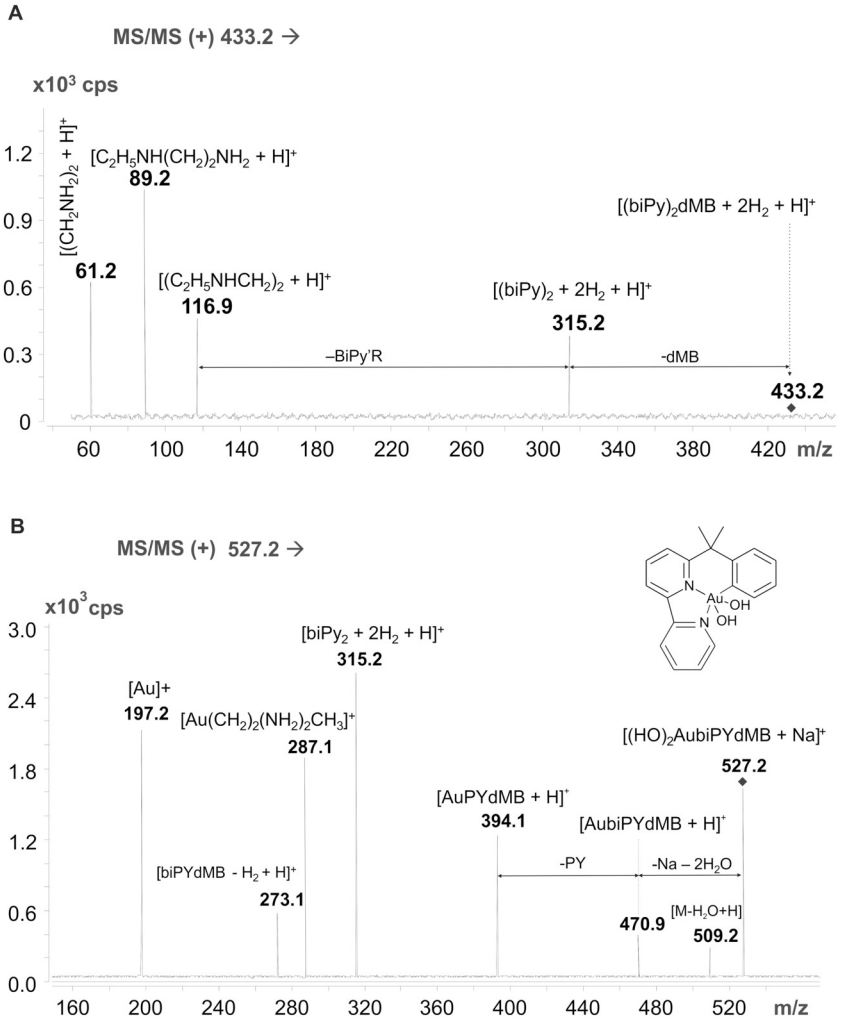

Fig. 6. EC/ESI-MS^2 mass spectra for ions m/z 433 (A) and m/z 527 (B) obtained for Aubipy^c.

Table 3
Proposed identities for signals observed by EC/ESI-MS for Aubipy^c complex.

Complex of Au(III), [Au = biPYisoPB(OH)]$^+PF_6^-$, M_{ml} = 634.32; Au = biPYisoPB(OH), M_{ml} = 487.1

m/z	Fragmentation ions	Proposed formula	M^*_{exp}	$M^*_{theor.}$	ΔM [ppm]
Zone I (−1.3–1.3 V)					
+433	61, 89, 117, 257, 251, 315	$[(biPY)_2isoPB + H_2 + H^+]^+$	432.18	432.12	41
+364	197, 273, 287	$[Au^I\text{-}PYMB]^+$	364.14	364.04	275
+226	197	$[Au^I\text{-}CH{=}NH + H^+]^+$	225.00	224.98	89
+157	80	$[biPY + H^+]^+$	156.10	156.07	191
Zone II (1.3–3.5 V)					
+527	197, 273, 287, 315, 394, 471, 509	$[Au^{III}\text{-}biPYisoPB(OH)_2 + Na^+]^+$	504.21	504.13	158
+517	197, 273, 287, 315, 394, 471	$[Au^{III}\text{-}biPYisoPB(OH)(CH{=}NH) + H^+]^+$	516.25	516.13	188
+273	80, 157	$[biPYisoPB - H_2 + H^+]^+$	272.20	272.13	256

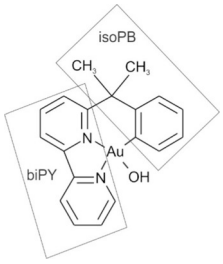

biPY – bipyridine, PY - pyridine, isoPB – isopropylobenzen; MB – methylbenzen,
ΔM – established as a ratio $|M^*_{exp.}\text{-}M^*_{theorit.}|/M^*_{theorit.}$
*Monoisotopic mass of molecule

to many mass voltammograms obtained for Auranofin. Those disturbances were usually observed when hydrolysis of complex enhanced by sodium ion took place. It can be concluded that signal oscillations observed in the EC/ESI-MS voltammograms reflect the influence of secondary reactions such as modification of the ligand (deacetylation) or ligand exchange (hydrolysis or attachment of nitrile ion) accompanying the redox one [42].

4. Conclusion

We have shown here that the EC/ESI-MS method allows to study the redox transformations of transition metal complexes and can be considered as a valuable complementary technique to other electrochemical methods. Moreover, ESI-MS detection allows tracking additional reactions such as hydrolysis or ligand exchange. As a result, the quality of MS voltammograms is higher for the more stable complexes. EC/ESI-MS offers insight into transformations of both the metal center and the ligand during the electrochemical process. Metal reduction changes the coordination number and affinity to ligands. In the case of ligands, redox reactions resulted in loss or formation of new C—C or S—S bound. It was also possible to identify the nitrile group as a nucleophilic ligand with high affinity for gold ions. When attached to Au (I) or Au(III) ions the nitrile group efficiently stabilized the complex and inhibited redox reactions (oxidation of tetraAtgS) or hydrolysis. Auranofin was found to be irreversibly oxidized, whereas the gold(III) complex, Aubipy^c, was found to be activated by ligand exchange combined with reduction of the gold(III) center in the electrochemical potential range corresponding to that of blood and cytosol.

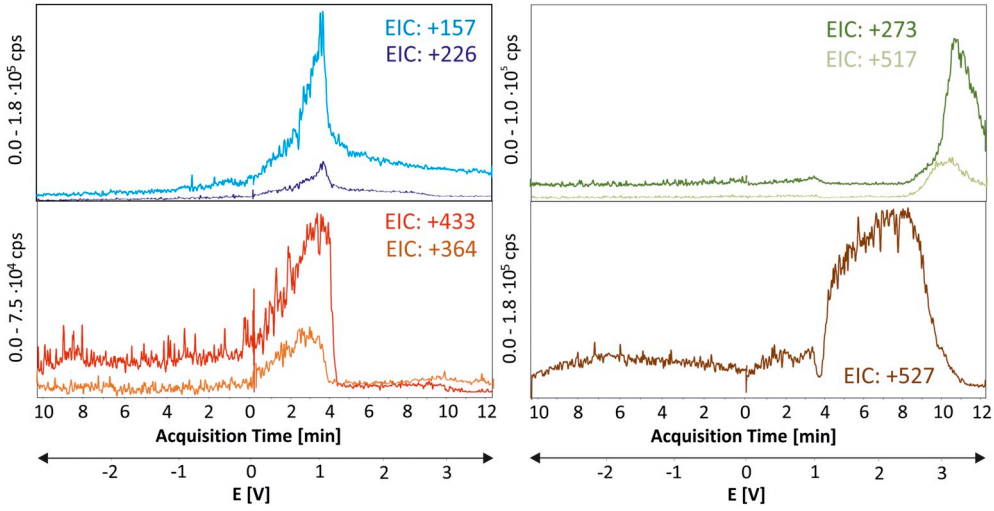

Fig. 7. Mass spectrometric voltammograms of selected ions (not smoothed extracted ion chromatograms, EICs) obtained by EC/ESI-MS for 10 μM Aubipy^c in the mixture of 10 mM ammonium formate pH 7.4 in water and ACN (70:30).

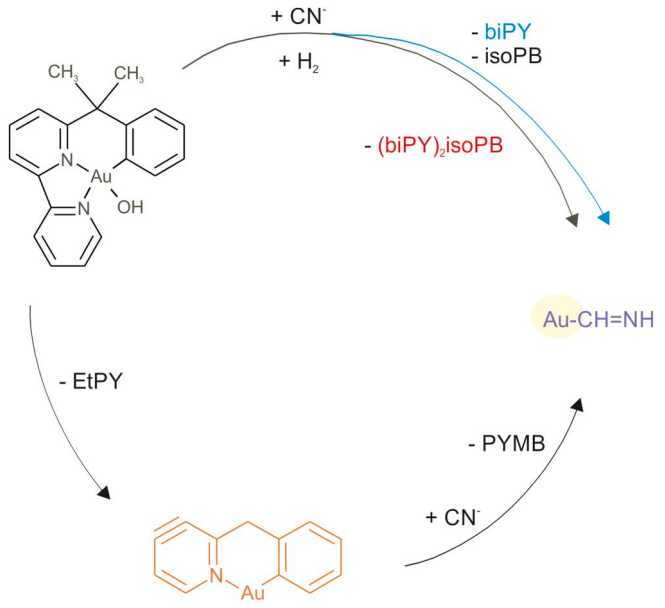

Fig. 8. Transformation of Aubipy^{c} obtained by EC/ESI-MS. Au(I) ion with the yellow background is proposed as the most probable active form of an investigated prodrug. Colors of drawings correspond to colors of mass spectrometric voltammograms present in Fig. 7. (For interpretation of the references to color in this figure legend, the reader is referred to the web version of this article.)

Abbreviations

Aubipy^{c}	[Au(bipy^{dmb}-H)(OH)][PF_6] where (bipy^{dmb} = 6-(1,1-dimethylbenzyl)-2,2′-bipyridine)
Auranofin	2,3,4,6-tetra-*o*-acetyl-L-thio-β-D-glyco-pyranosato-S-(triethyl-phosphine)gold(I)
biPY	bipyridine
EC	electrochemical reaction cell
EC/ESI-MS	coupling of electrochemical reaction cell with electrospray ionization mass spectrometry
EIC	extraction of ion chromatograms
ESI-MS	electrospray ionization mass spectrometry
isoPB	isopropylobenzen
MB	methylbenzene
PY	pyridine
SWV	square wave voltammetry
tEP	triethylphosphanium group
tetraAtgS	tetraacetyl-1-thio-β-D-glucopyranosato-S group
tri/diA	tri/diacetyl group

Acknowledgments

The authors thank Shim-pol company for providing instrumentation necessary for electrochemical experiments, Marcin Gawryś, Tomasz Moździński and Wojciech Wróblewski for worthwhile remarks.

Funding sources

The research was financially supported by Warsaw University of Technology and the Polish National Center of Science (NCN) in the frame of the project DEC-2013/09/B/ST4/00961.

Notes

The authors declare no competing financial interest.

Author contributions

The manuscript was written through the contributions of all authors. All authors have given approval to the final version of the manuscript.

References

[1] M.P.M. Marques, ISRN Spectrosc. 2013 (2013) 1–29.
[2] S.H. van Rijt, P.J. Sadler, Drug Discov. Today 14 (2009) 1089–1097.
[3] C.G. Hartinger, P.J. Dyson, Chem. Soc. Rev. 38 (2009) 391–401.
[4] S. Nobili S, E. Mini, I. Landini, C. Gabbiani, A. Casini, L. Messori, Med. Res. Rev. 30 (2010) 550–580.
[5] F. Hassan, D.T. Al-Aridhi, Int. J. Pharma Sci. 5 (2015) 1317–1322.
[6] R. Padmanabha, K.B. Chandrasekhar, J.S. Mohammed, Pharm. Res. 7 (2015) 193–197.
[7] J.L. Larabee, J.R. Hocker, J.S. Hanas, Chem. Res. Toxicol. 18 (2005) 1943–1954.
[8] I. Romero-Canelón, P.J. Sadler, Inorg. Chem. 52 (2013) 12276–12291.
[9] R. Milo, R. Phillips, Cell Biology by the Numbers, Garland Science, New York, 2015.
[10] M.Sh. Khubutiya, A.K. Evseev, V.A. Kolesnikov, M.M. Goldin, A.D. Davydov, A.G. Volkov, A.A. Stepanov, Russ. J. Electrochem. 46 (2010) 537–541.
[11] Y.N. Gavhane, A.V. Yadav, Saudi Pharm. J. 20 (2012) 331–344.
[12] R. Holmgaard, J.B. Nielsen, E. Belnfeld, Skin Pharmacol. Physiol. 23 (2010) 225–243.
[13] K. Krumova, G. Cosa, S. Nonell, C. Flors (Eds.), Singlet Oxygen: Applications in Biosciences and Nanosciences, vol. 1, The Royal Society of Chemistry, Cambridge, 2016, pp. 1–21.
[14] J. Wang, Analytical Electrochemistry, John Wiley and Sons, New Jersey, 2006.
[15] H.-L. Wu, C. Kang, Y. Li, R.-Q. Yu, A.M. de la Peña, H.C. Goicoechea, G.M. Escandar, A.C. Olivieri (Eds.), Data Handling in Science and Technology, vol. 29, Elsevier, Amsterdam, 2015, pp. 167–246.
[16] C. Zettersten, M. Co, S. Wende, C. Turner, L. Nyholm, P.J. Sjöberg, Anal. Chem. 81 (2009) 8968–8977.
[17] P.F. Oberacher, R. Erb, S. Plattner, Mass Spectrom. Rev. 34 (2015) 64–92.
[18] D.T. Hill, B.M. Sutton, Cryst. Struct. Commun. 9 (1980) 679–686.
[19] C. Roder, M.J. Thomson, Drugs R&D 15 (2015) 13–20.
[20] H. Guo-Xin, L. Pan-Pan, Z. Shengyi, Y. Mengqi, L. Jianwei, Y. Jing, H. Yumin, J. Wen-Qi, W. Shijun, H. Peng, Cell Death Dis. 89 (2018) 1–15.
[21] J.L. Roh, H. Jang, E.H. Kim, D. Shin, Antioxid. Redox Signal. 27 (2017) 106–114.
[22] U. S. National Liabrary of Medicine, Auranofin in treating patients with recurrent epithelial ovarian, primary peritoneal, or fallopian tube cancer, https://clinicaltrials.gov/ct2/show/NCT01747798, (2015) , Accessed date: 18 March 2019.
[23] U. S. National Liabrary of Medicine, Sirolimus and auranofin in treating patients with advanced or recurrent non-small cell lung cancer or small cell lung cancer, https://clinicaltrials.gov/ct2/show/NCT01737502, (2019) , Accessed date: 18 March 2019.
[24] U. S. National Liabrary of Medicine, Phase I and II study of auranofin in chronic lymphocytic leukemia (CLL), https://clinicaltrials.gov/ct2/show/NCT01419691, (2015) , Accessed date: 18 March 2019.
[25] G. Marcon, S. Carotti, M. Coronnello, L. Messori, E. Mini, P. Orioli, T. Mazzei, M.A. Cinellu, G. Minghetti, J. Med. Chem. 45 (2002) 1672–1677.
[26] C. Gabbiani, M.A. Cinellu, L. Maiore, L. Massai, F. Scaletti, L. Messori, Inorg. Chim. Acta 393 (2012) 115–124.
[27] A. Casini, G. Kelter, C. Gabbiani, M.A. Cinellu, G. Minghetti, D. Fregona, H.H. Fiebig, L. Messori, J. Biol. Inorg. Chem. 14 (2009) 1139–1149.
[28] T. Gamberi, L. Massai, F. Magherini, I. Landini, T. Fiaschi, F. Scaletti, C. Gabbiani, L. Bianchi, L. Bini, S. Nobili, G. Perrone, E. Mini, L. Messori, A. Modesti, J. Proteome 103 (2014) 103–120.
[29] G.J. van Berkel, F. Zhou, Anal. Chem. 67 (1995) 2916–2923.
[30] P.A. Kohl, M. Schlesinger, M. Paunovic (Ed.), Modern Electroplating, John Wiley & Sons, New Jersey, 2010, pp. 115–130.
[31] A. Albert, C. Brauckmann, F. Blaske, M. Sperling, C. Engelhard, U. Karst, J. Anal. At. Spectrom. 27 (2012) 975–981.
[32] R. Gulaboski, J. Solid State Electrochem. 13 (2009) 1015–1024.
[33] R. Gulaboski, L. Mihajlov, Biophys. Chem. 155 (2011) 1–9.
[34] K. Pawlak, W. Jakubczak, Bioanalysis 6 (2014) 273–276.
[35] A.R. Ross, M.G. Ikonomou, K.J. Orians, J. Mass Spectrom. 35 (2000) 981–989.
[36] A.J. Kell, D.L.B. Stringle, M.S. Workentin, Org. Lett. 21 (2000) 3381–3384.
[37] N.K. Chaki, Y. Negishi, H. Tsunoyama, Y. Shichibu, T. Tsukuda, J. Am. Chem. Soc. 130 (2008) 8608–8610.
[38] A.A. Mohamed, J. Chen, A.E. Bruce, M.R.M. Bruce, J.A. Bauer, D.T. Hill, Inorg. Chem. 42 (2003) 2203–2205.
[39] F.J. Owens, Int. J. Quantum Chem. 117 (2017) e25347–e25356.
[40] R.A. de Graaf, G.A. Broekroelof, L.P.B.M. Janssen, A.A.C.M. Beenackers, Carbohydr. Polym. 28 (1995) 137–144.
[41] L.D. Burke, P.F. Nugent, Gold Bull. 30 (1997) 43–53.
[42] L. Mercs, A. Neels, M. Albrecht, Dalton Trans. 41 (2008) 5570–5576.